Journal of Power Sources 195 (2010) 7146–7151

Contents lists available at ScienceDirect

Journal of Power Sources

journal homepage: www.elsevier.com/locate/jpowsour

Hollow carbon hemispheres supported palladium electrocatalyst at improved performance for alcohol oxidation

Zaoxue Yan [a], Zhuofeng Hu [a], Chan Chen [a], Hui Meng [a], Pei Kang Shen [a,*], Hongbin Ji [b], Yuezhong Meng [a,**]

[a] The Key Laboratory of Low-carbon Chemistry & Energy Conservation of Guangdong Province, The State Key Laboratory of Optoelectronic Materials and Technologies, Sun Yat-sen University, Guangzhou 510275, PR China
[b] School of Chemistry and Chemical Engineering, The Key Laboratory of Low-carbon Chemistry & Energy Conservation of Guangdong Province, Sun Yat-sen University, Guangzhou 510275, PR China

ARTICLE INFO

Article history:
Received 2 April 2010
Received in revised form 3 June 2010
Accepted 3 June 2010
Available online 9 June 2010

Keywords:
Hollow carbon hemisphere
Fuel cell
Ethanol oxidation
Palladium electrocatalyst

ABSTRACT

The synthesis procedure of the hollow carbon hemispheres (HCHs) using glucose as carbon source and polystyrene spheres (PSs) as templates and the formation mechanism of the HCHs have been presented. The HCHs have regular morphology and high BET surface area of 702.7 $m^2 g^{-1}$. The advantage of the HCHs compared to the hollow carbon spheres is that the HCHs can provide similar surface area at reduced volume. The electrocatalytic activity of ethanol oxidation on Pd supported on HCHs electrocatalyst (Pd/HCH) is 2.8 times higher than that of Pd supported on commercial Vulcan XC-72 carbon (Pd/C) electrocatalyst at the same Pd loadings. The high surface area is beneficial for the dispersion of the precious metal nanoparticles to increase their utilization. The hemispherical structure with hollow shell results in the improvement in the mass transfer and therefore more concentrated ethanol solution can be used to increase the energy density.

1. Introduction

Various carbon materials such as carbon nanotubes [1–3], carbon nanospheres [4,5], carbon nanowires [6–8], carbon nanofibers [9–11], porous carbon [12], fullerene [13], graphene [14], diamond-like carbon [15,16], glass-like carbon [17], onion-like carbon [18], honeycomb-like carbon [19], coin-like carbon [20] and hollow carbon spheres [21,22] have been synthesized in recent years. Those carbon materials showed high surface area, low density, high chemical stability and excellent electrical conductivity. Therefore, they are extensively applied as catalyst support [23–27], adsorbent [28,29], energy storage [30,31], microelectrode [32] and wireless realm [33] and so on. As electrocatalyst supports, they provide special structures (morphologies) to well disperse metal nanoparticles and improve the mass transfer. Various carbon materials have been prepared in our group as noble metal supports for alcohol electrooxidation and oxygen reduction reaction at an improved performance [19,34–41]. Here, we report for the first time the synthesis of hollow carbon hemispheres (HCHs) with glucose as carbon source and polystyrene spheres (PSs) as templates. By comparing to hollow carbon spheres (HCSs), such structured carbon materials can provide high surface area at reduced volume. Pd supported on HCHs as electrocatalysts were tested for alcohol oxidation in alkaline media [42–46].

2. Experimental

2.1. Preparation of the HCHs

PSs were often used as templates for preparing hollow metal oxide, hollow composite spheres and hollow carbon spheres [38,47–49]. In this study, the PSs were obtained by emulsifier-free emulsion polymerization method. Typically, 1.0 g PSs, 2.0 g glucose and 40 ml deionized water were mixed in a 50 ml autoclave and heated at 160 °C for 15 h. The product was then washed with deionized water and ethanol and dried at 90 °C for 1 h. Afterwards, the dried product was heated in a homemade program-controlled microwave oven (1000 W, 2.45 GHz) by an intermittent microwave heating (IMH) procedure of 80 s on and 60 s off and 80 s on again. Finally, the product was carbonized at 900 °C for 3 h in nitrogen atmosphere to get hollow carbon hemispheres (HCHs).

2.2. Preparation of Pd/HCH electrocatalysts

Pd supported on the HCHs (denotes as Pd/HCH) or carbon powders (denotes as Pd/C) were prepared and used for alcohol oxi-

* Corresponding author at: School of Physics and Engineering, Sun Yat-sen University, 135 Xingang Road, Guangzhou 510275, Guangdong, PR China. Tel.: +86 20 84036736; fax: +86 20 84113369.
** Corresponding author. Tel.: +86 20 84036736; fax: +86 20 84113369.
E-mail addresses: stsspk@mail.sysu.edu.cn (P.K. Shen), mengyzh@mail.sysu.edu.cn (Y. Meng).

0378-7753/$ – see front matter © 2010 Elsevier B.V. All rights reserved.
doi:10.1016/j.jpowsour.2010.06.014

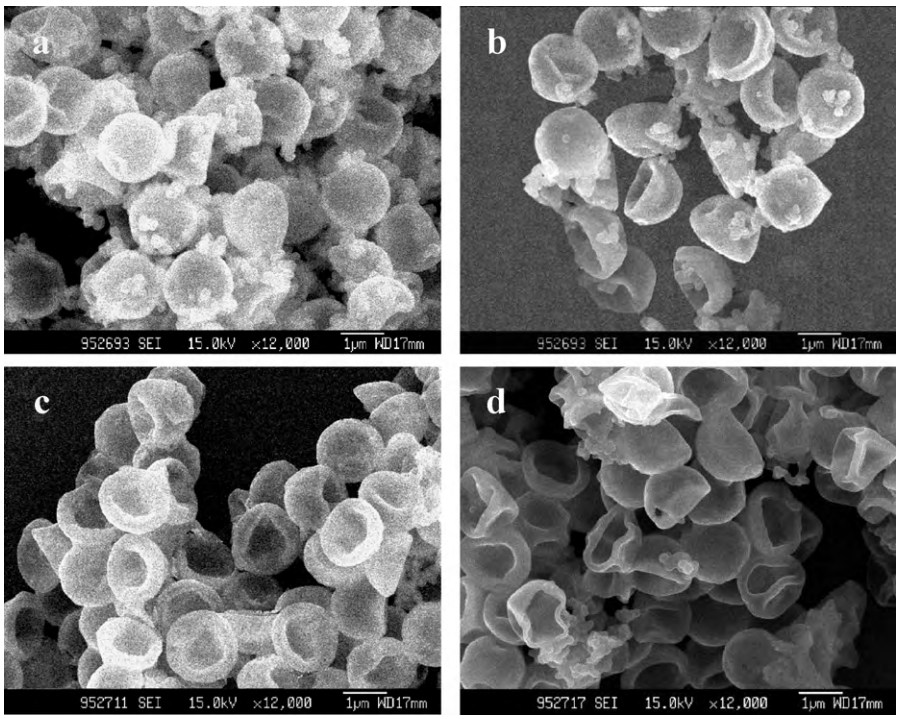

Fig. 1. SEM micrograms of the HCHs with the mass ratios of PSs to glucose were (a) 1:4, (b) 1:3, (c) 1:2 and (d) 1:1.

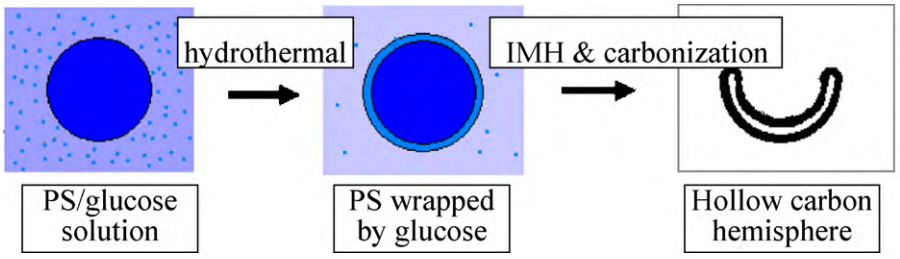

Scheme 1. Schematic illustration of the synthesis procedure of the HCHs.

dation. Typically, HCHs or Vulcan XC-72 carbon (50 mg) was added into the mixture of 16.67 mg $PdCl_2$ and 50 ml glycol and dispersed to uniform ink in ultrasonic bath for 30 min. The pH of the mixture was then adjusted to 10 by 5 wt% NaOH/glycol solution and put into a homemade program-controlled microwave oven (1000 W, 2.45 GHz) for heating at a 10 s on and 10 s off procedure for 10 times. Afterwards, the mixture was washed with water for 4–5 times and dried in vacuum at 80 °C for 2 h. The Pd loadings on the electrocatalysts were 20 wt%.

For electrode preparation, 5 mg Pd/HCH or Pd/C were dispersed in 1 ml ethanol and 1 ml 0.5 wt% Nafion suspension (DuPont, USA) under ultrasonic agitation to form the electrocatalyst ink. The electrocatalyst ink (40 μl) was then deposited on the surface of the glassy carbon rod and dried at room temperature overnight. The total Pd loadings were controlled at 0.02 mg cm^{-2}.

All chemicals were of analytical grade and used as received.

2.3. Characterization of HCHs and Pd/HCH electrocatalysts

All electrochemical measurements were performed in a three-electrode cell on an IM6e potentiastat (Zahner-Electrik, Germany) at 30 °C controlled by a water-bath thermostat. A platinum foil (1.0 cm^2) and Hg/HgO (1.0 mol dm^{-3} KOH) were used as counter and reference electrodes, respectively.

The structures of the materials were determined on an X-ray diffractometer (CuK1, λ = 1.54056 Å, D/Max-IIIA, Rigaku Co., Japan). The BET surface area, pore volume and pore diameter were determined on a Physical Adsorption Instrument (ASAP 2400, Micrometeritics Co., USA). The morphology and size of Pd/HCH or Pd/C electrocatalysts were characterized by scanning electron microscopy (SEM, LEO 1530VP, Germany) and a JOEP JEM-2010 (JEOL Ltd.) transmission electron microscopy (TEM) operating at 200 kV.

3. Results and discussion

Fig. 1 shows the SEM micrograms of the HCHs. It is clear that the formation of HCHs depends on the ratio of the PSs and glucose. Fig. 1a–c shows the mixtures of spheres and hemispheres with the different percentages. The percentage of the HCHs increases with decrease in the glucose as shown in Table 1. However, almost pure HCHs can be obtained at the mass ratio of PSs to glucose of 1:1 but some of them were deformed as shown in Fig. 1d. The size of the

Table 1
Effect of the ratio of PSs to glucose on the percentage of the HCHs.

The mass ratio of PS to glucose	1:4	1:3	1:2
The percentage of HCHs (%)	~30	~70	>90

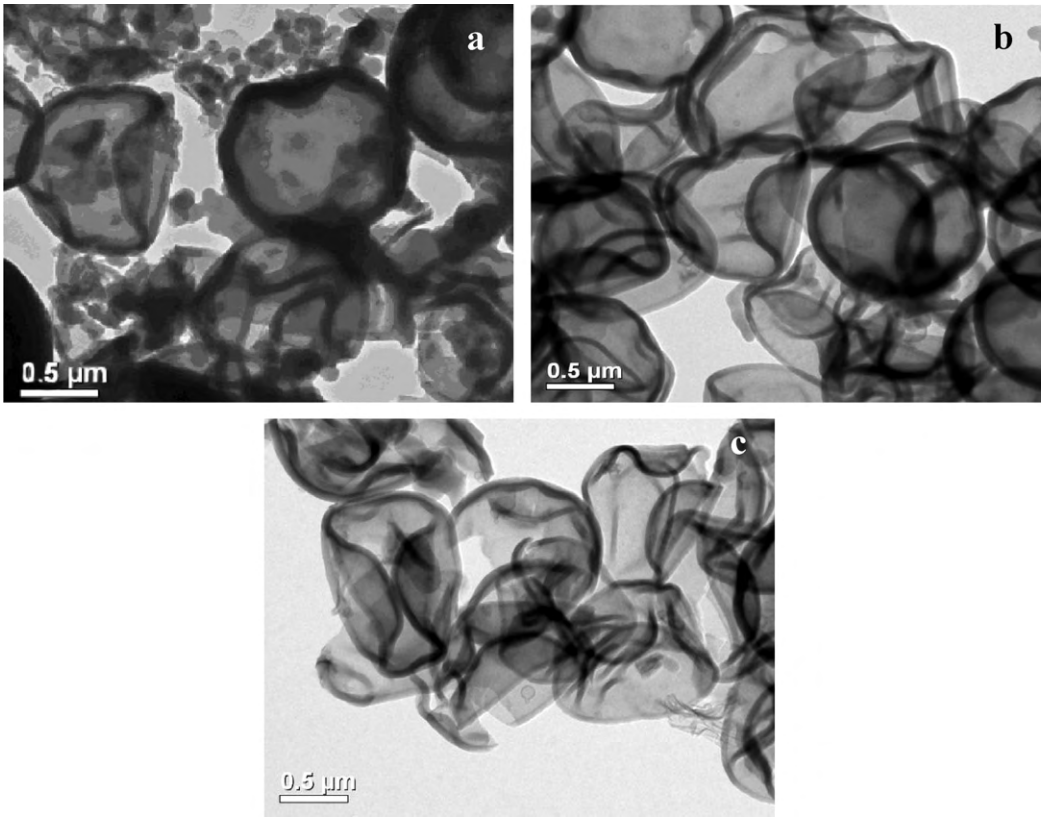

Fig. 2. TEM images of the HCHs formed at the mass ratios of PSs to glucose (a) 1:3, (b) 1:2 and (c) 1:1.

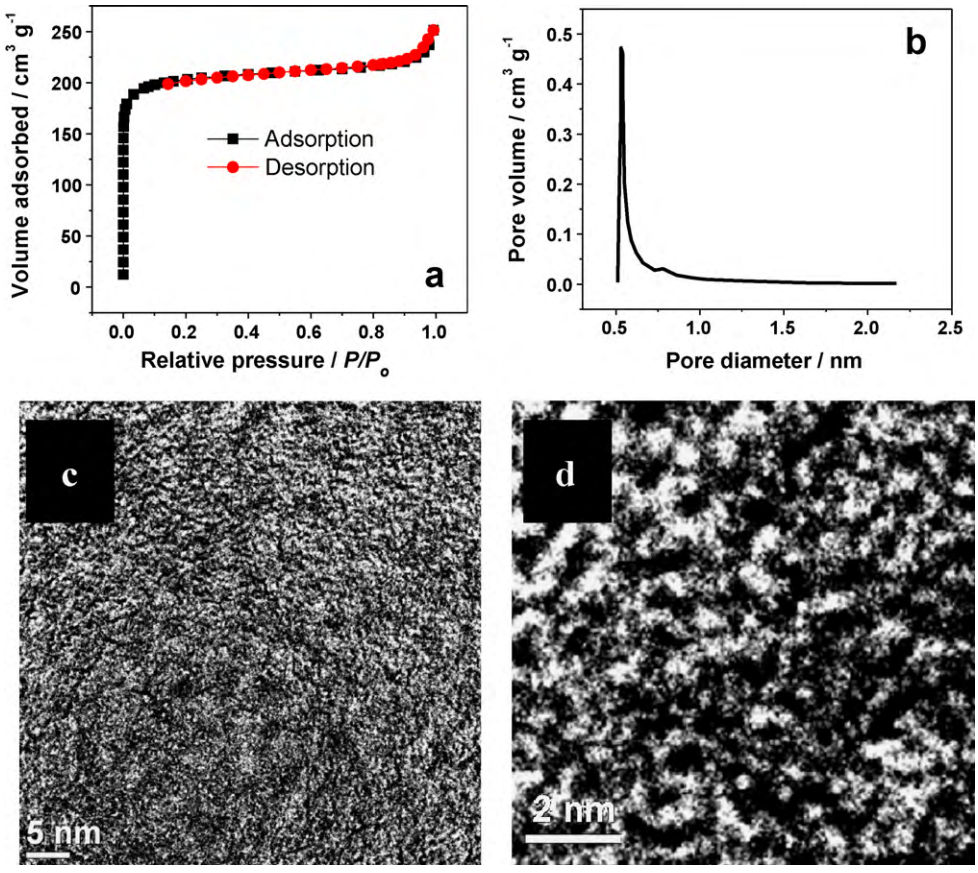

Fig. 3. (a) N_2 adsorption and desorption isotherm, (b) pore size distribution, (c and d) HRTEM images of HCHs (PSs:glucose (mass ratio) = 1:2).

Table 2
BET analysis data of HCHs.

PS:glucose (mass ratio)	Total surface area ($m^2\ g^{-1}$)	Micropore area ($m^2\ g^{-1}$)	Total pore volume ($cm^3\ g^{-1}$)	Micropore volume ($cm^3\ g^{-1}$)
1:4	664.7	583.3	0.35	0.27
1:3	702.7	564.0	0.39	0.26
1:2	733.4	547.4	0.42	0.25

HCHs depends on the size of PSs. The smaller the PSs the smaller the HCHS are, indicating that the size of the HCHs is tunable.

The synthesis procedure of HCHs is schematically illustrated in Scheme 1. The first step is to mix glucose, water and PSs for the hydrothermal reaction. The PSs are wrapped by glucose and partially carbonized during the hydrothermal reaction processes. The second step is to remove the PSs by IMH treatment in air. The glucose layer is carbonized along with the pyrolysis of PSs. Finally, the thin-walled hollow carbon spheres (HCSs) cave into hollow carbon hemispheres after the removal of PSs. The hollow carbon hemispherical structure would not reduce the surface area but can significantly reduce the volume compared to the hollow carbon spheres.

The TEM images as shown in Fig. 2 further prove the formation of HCHs due to the cave-in of the thin-walled HCSs. At higher glucose percentage, the products formed with thicker carbon wall that results in the products dominated with HCSs. With the increase in the percentage of PSs, the walls of the hollow carbon spheres become thinner and finally cave-in into HCHs. Moreover, deformed HCHs formed at even lower glucose percentage as shown in Fig. 2c.

The N_2 adsorption and desorption isotherm (Fig. 3a) and pore size distribution (Fig. 3b) indicated that the dominant pores on

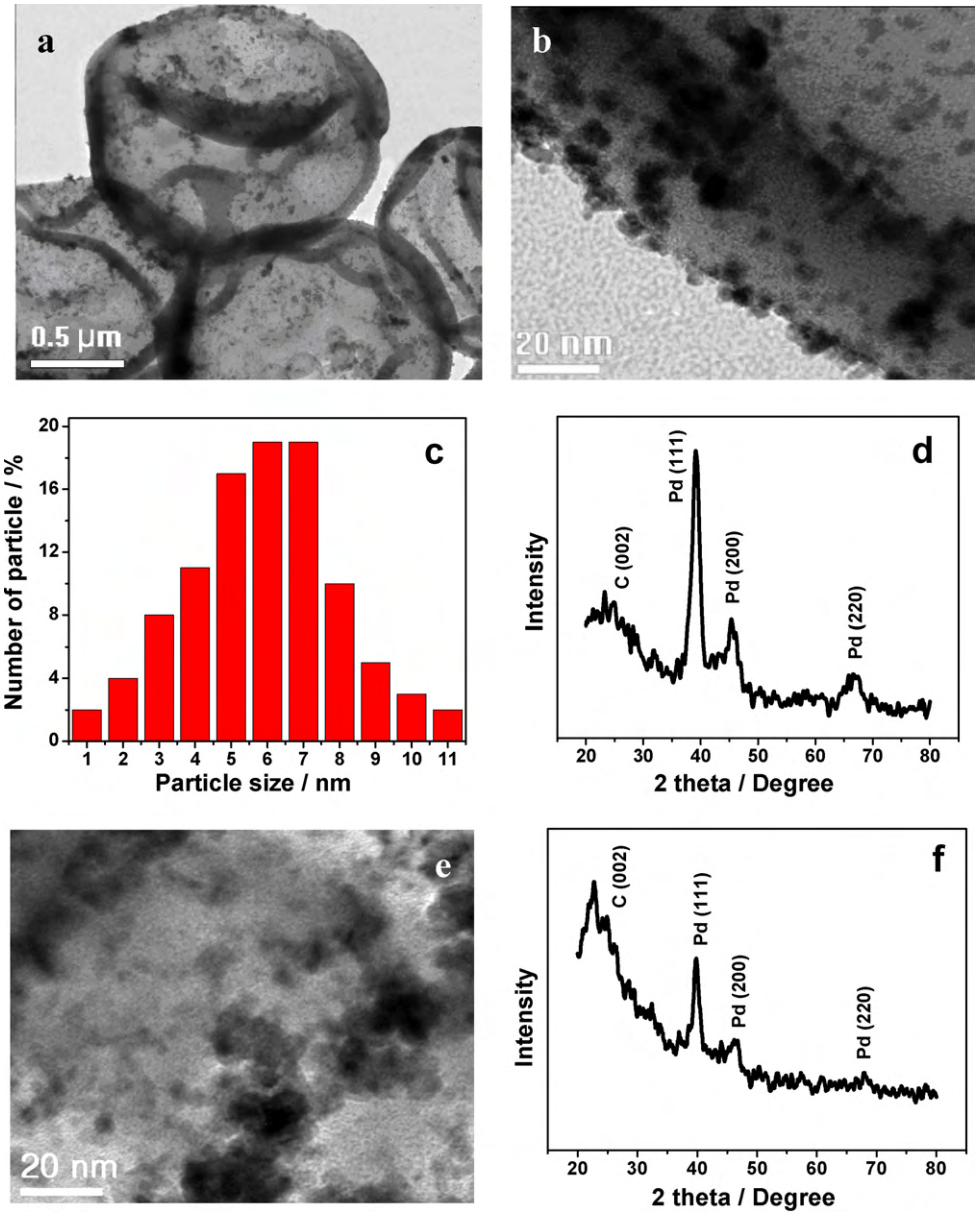

Fig. 4. (a) TEM image of Pd/HCH (bar 500 nm), (b) HRTEM image of Pd/HCH (bar 20 nm), (c) corresponding particle size distribution of Pd/HCH, (d) XRD pattern of Pd/HCH, (e) TEM image of Pd/C (bar 20 nm) and (f) XRD pattern of Pd/C.

HCHs were micropores. Fig. 3c and d shows the HRTEM images of HCHs (corresponding to Fig. 2b) with large amounts of micropores, which contributes to its large micropore area and large micropore volume. Table 2 summarizes the BET surface area, pore volume and pore diameter of the HCHs with different PSs to glucose ratios. With the decreasing in the amounts of glucose, the total surface area and total pore volume increase, while the micropore area and micropore volume decrease. The reason is simple. At lower glucose percentage, the walls of the formed carbon spheres are thinner and the more micropores existed after the carbonization. While at higher glucose percentage, the walls of the formed carbon spheres are thicker and more micropores are blocked, resulting in reduction in the micropore area and micropore volume.

The HCHs prepared at 1:2 mass ratio of PSs to glucose were used as support to load Pd nanoparticles for alcohol oxidation. Fig. 4a and b shows the uniform distribution of Pd nanoparticles supported on the HCHs. The corresponding histogram (Fig. 4c) indicates a Gaussian distribution of Pd nanoparticle size with the average particle size of 5.9 nm based on 100 Pd particles randomly selected from the HRTEM image as shown in Fig. 4b. Fig. 4d shows the XRD pattern of the Pd/HCH electrocatalyst. The diffraction peak at 2θ of 23.2° was observed which corresponds to (0 0 2) facet of the graphitic carbon, indicating that the HCHs were partially graphitized from the amorphous nature. The diffraction peaks at 2θ of 39.4°, 45.1° and 66.6° correspond to the (1 1 1), (2 0 0) and (2 2 0) facets of the face-centered cubic structure of palladium crystal. The Pd (2 2 0) peak was used to calculate the particle size according to the Scherrer's equation.

$$D = \frac{K\lambda}{B\cos q}$$

where D denotes the average diameter in nm, K the Scherrer constant (0.89), k the wavelength of X-ray (k = 0.154056 nm), B the corresponding full width at half maximum (FWHM) of the (2 2 0) diffraction peak and θ the Bragg's diffraction angle. The calculated Pd particle size was 5.7 nm which is consistent with the TEM

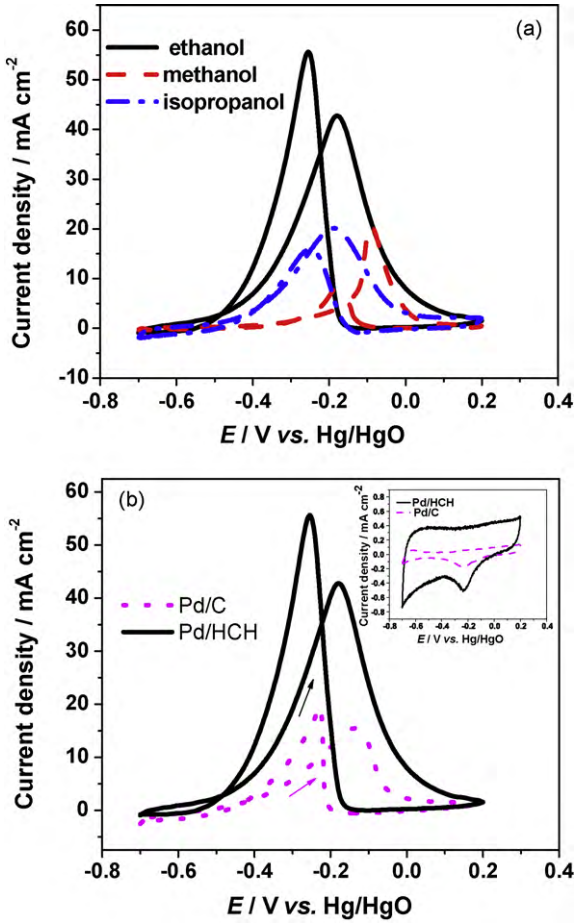

Fig. 5. Cyclic voltammograms of (a) different alcohol oxidation on Pd/HCH electrode and (b) ethanol oxidation on Pd/HCH and Pd/C electrodes in 1.0 mol dm^{-3} KOH/1.0 mol dm^{-3} alcohol solution at 303 K, scan rate: 50 mV s^{-1}. The inset in (b) is the cyclic voltammograms of Pd/HCH and Pd/C in 1.0 mol dm^{-3} KOH solution at 303 K, scan rate: 50 mV s^{-1}.

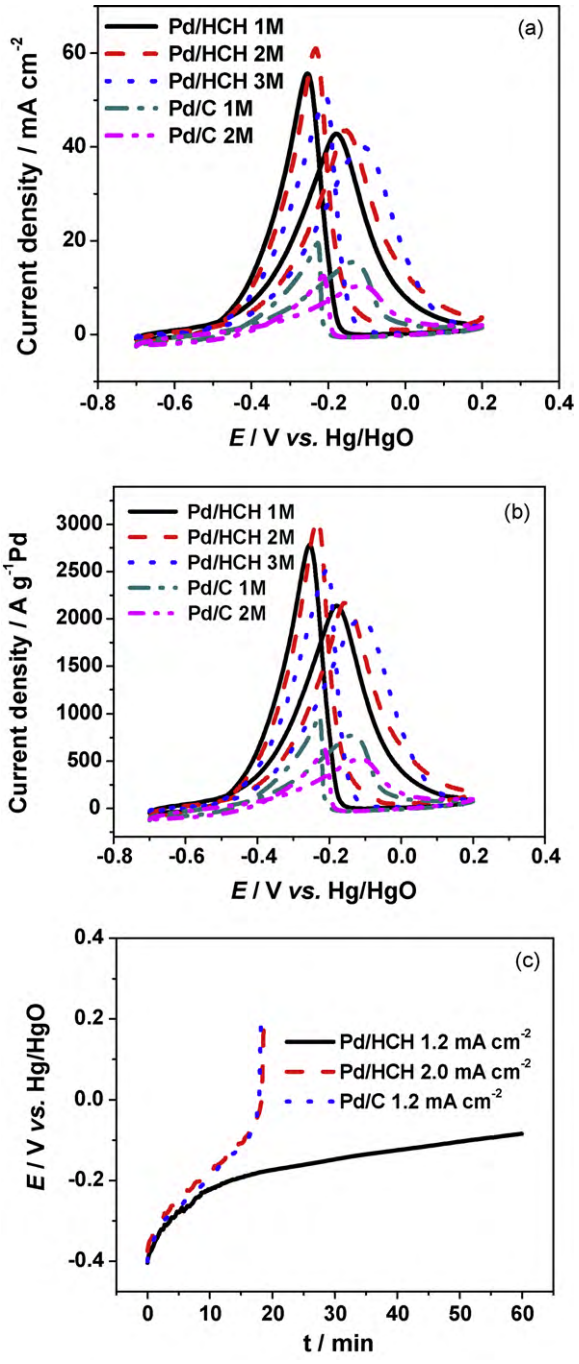

Fig. 6. (a) Cyclic voltammograms of ethanol oxidation on Pd/C and Pd/HCH in 1.0 mol dm^{-3} KOH containing different ethanol concentration at 303 K, scan rate: 50 mV s^{-1}, (b) the mass activity–potential curves made by the same data as shown in (a), and (c) chronopotentiometric curves of ethanol oxidation on Pd/C and Pd/HCH at different current densities in 1.0 mol dm^{-3} ethanol/1.0 mol dm^{-3} KOH solution, 303 K.

results. The TEM image of Pd/C (Fig. 4e) displays the dispersion of Pd nanoparticles with partial aggregation. The average particle size was 6.4 nm based on 50 Pd particles randomly selected. The particle size calculated the XRD pattern of Pd/C (Fig. 4f) to be 7.0 nm by Scherrer's equation, which is very close to the TEM results.

Fig. 5a shows the cyclic voltammograms of ethanol, methanol and isopropanol oxidation on Pd/HCH electrodes. The Pd/HCH electrocatalyst shows extremely high activity for the ethanol oxidation in terms of the onset potential and peak current density in comparison with methanol and isopropanol in alkaline solution. Moreover, the Pd/HCH shows peak current density for ethanol oxidation of 2.8 times as high as that on Pd/C electrocatalyst at the same Pd loadings. The results proved that the use of HCHs significantly improved the dispersion and utilization of the precious metal nanoparticles, which were further evidenced by comparing the electrochemical active surface area as shown in the inset of Fig. 5b. The Pd/HCH shows much higher electrochemical active surface area than that of Pd/C. Furthermore, it is obvious that the hemisphere structure of the HCHs as support definitely improves the mass transfer for the electrochemical reactions compared to the carbon powder support. This is extremely important for the liquid fuel cells like direct alcohol fuel cells.

The improved mass transfer property of the Pd/HCH electrocatalyst was evidenced for ethanol oxidation in more concentrated ethanol solution. The Pd/C electrode showed a maximum current density in 1 mol dm^{-3} ethanol solution as shown in Fig. 6a. However, the Pd/HCH electrode gave the maximum current density in 2 mol dm^{-3} ethanol solution. As shown in Fig. 6b that the mass activity of the ethanol oxidation in 2 mol dm^{-3} ethanol solution was 2200 A g^{-1} Pd which is much higher than that of 750 A g^{-1} Pd on Pd/C electrode. The results are important for direct alcohol fuel cells since the use of concentrated alcohol solution would significantly increase the energy density and reduce both weight and volume. The chronopotentiometric testing proved that the Pd/HCH electrocatalyst could sustain larger current densities for stable ethanol oxidation than that of Pd/C electrocatalyst as shown in Fig. 6c at the same Pd loadings.

4. Conclusions

Hollow carbon hemispheres (HCHs) were prepared using glucose as carbon source and polystyrene spheres (PSs) as templates. The HCHs show extremely high surface area of 702.7 $m^2 g^{-1}$ according to the N_2 adsorption/desorption measurement and an average pore diameter of about 2.29 nm determined by BJH method. The high surface area and the mesoporous structure are beneficial for the uniform dispersion of the precious metal nanoparticles to increase their utilization. The current densities on Pd/HCH electrocatalyst for ethanol oxidation were 2.8 times as many as that on Pd supported on commercial Vulcan XC-72 carbon (Pd/C) electrocatalyst at the same Pd loadings. The hemispherical structure with hollow shell results in the improvement in the mass transfer and therefore more concentrated ethanol solution can be used to increase the energy density.

Acknowledgement

The work was supported by the China National 863 Program (2009AA05Z110).

References

[1] M.X. Tang, Y.J. Qin, Y.Y. Wang, Z.X. Guo, J. Phys. Chem. C 113 (2009) 1666–1671.
[2] D. Takagi, H. Hibino, S. Suzuki, Y. Kobayashi, Y. Homma, Nano Lett. 7 (2007) 2272–2275.
[3] K. Koziol, J. Vilatela, A. Moisala, M. Motta, P. Cunniff, M. Sennett, A. Windle, Science 318 (2007) 1892–1895.
[4] Y. Li, J.F. Chen, Q. Xu, L.H. He, Z.M. Chen, J. Phys. Chem. C 113 (2009) 10085–10089.
[5] Y. Wang, F.B. Su, C.D. Wood, J.Y. Lee, X.S. Zhao, Ind. Eng. Chem. Res. 47 (2008) 2294–2300.
[6] H. Li, F.W. Sun, Y.F. Li, X.F. Liu, K.M. Liew, Scripta Mater. 59 (2008) 479–482.
[7] H.W. Seo, C.S. Han, W.S. Jang, J. Park, Curr. Appl. Phys. 6S1 (2006) e216–e219.
[8] W. Wang, K. Yang, J. Gaillard, P.R. Bandaru, A.M. Rao, Adv. Mater. 20 (2008) 179.
[9] C.S. Lee, S.E. Baker, M.S. Marcus, W. Yang, M.A. Eriksson, R.J. Hamers, Nano Lett. 4 (2004) 1713–1716.
[10] A. Huczko, H. Lange, M. Sioda, Y.Q. Zhu, W.K. Hsu, H.W. Kroto, D.R.M. Walton, J. Phys. Chem. B 106 (2002) 1534–1536.
[11] F. Winter, V. Koot, A.J. Dillen, J.W. Geus, K.P. Jong, J. Catal. 236 (2005) 91–100.
[12] S.R.S. Prabaharan, R. Vimala, Z. Zainal, J. Power Sources 161 (2006) 730–736.
[13] H. Wang, R. DeSousa, J. Gasa, K. Tasaki, G. Stucky, B. Jousselme, F. Wudl, J. Membr. Sci. 289 (2007) 277–283.
[14] R. Prasher, Science 328 (2010) 185–186.
[15] A.P. Mousinho, R.D. Mansano, M.C. Salvadori, J. Alloy Compd. 495 (2010) 620–624.
[16] M. Moseler, P. Gumbsch, C. Casiraghi, A.C. Ferrari, J. Robertson, Science 309 (2005) 1545–1548.
[17] L.A. Pesin, E.M. Baitinger, Carbon 40 (2002) 295–306.
[18] P. Kuzhir, S. Maksimenko, D. Bychanok, V. Kuznetsov, S. Moseenkov, I. Mazov, O. Shenderova, P. Lambin, Metamaterials 3 (2009) 148–156.
[19] S.X. Chen, X. Zhang, P.K. Shen, Electrochem. Commun. 8 (2006) 713–719.
[20] D.S. Yuan, C.W. Xu, Y.L. Liu, S.Z. Tan, X. Wang, Z.D. Wei, P.K. Shen, Electrochem. Commun. 9 (2007) 2473–2478.
[21] Y. Wang, F.B. Su, J.Y. Lee, X.S. Zhao, Chem. Mater. 18 (2006) 1347–1353.
[22] G.D. Li, C.L. Guo, C.H. Sun, Z.H. Ju, L.S. Yang, L.Q. Xu, Y.T. Qian, J. Phys. Chem. C 112 (2008) 1896–1900.
[23] J.H. Bang, K. Han, S.E. Skrabalak, H. Kim, K.S. Suslick, J. Phys. Chem. C 111 (2007) 10959–10964.
[24] L. Li, G. Wu, B.Q. Xu, Carbon 44 (2006) 2973–2983.
[25] A. Lueking, R.T. Yang, J. Catal. 206 (2002) 165–168.
[26] M.L. Toebes, Y. Zhang, J. Hájek, T.A. Nijhuis, J.H. Bitter, A.J. Dillen, D.Y. Murzin, D.C. Koningsberger, K.P. Jong, J. Catal. 226 (2004) 215–225.
[27] Y.M. Liang, H.M. Zhang, H.X. Zhong, X.B. Zhu, Z.Q. Tian, D.Y. Xu, B.L. Yi, J. Catal. 238 (2006) 468–476.
[28] R. Quinn, T.A. Dahl, B.W. Diamond, B.A. Toseland, Ind. Eng. Chem. Res. 45 (2006) 6272–6278.
[29] V.Y. Yakovlev, A.A. Fomkin, A.V.J. Tvardovski, Colloid Interface Sci. 280 (2004) 305–308.
[30] J.W. Long, M.B. Sassin, A.E. Fischer, D.R. Rolison, A.N. Mansour, V.S. Johnson, P.E. Stallworth, S.G. Greenbaum, J. Phys. Chem. C 113 (2009) 17595–17598.
[31] C. Emmenegger, P. Mauron, P. Sudan, P. Wenger, V. Hermann, R. Gallay, A. Züttel, J. Power Sources 124 (2003) 321–329.
[32] J. Wang, R.P. Deo, P. Poulin, M. Mangey, J. Am. Chem. Soc. 125 (2003) 14706–14707.
[33] C. Rutherglen, P. Burke, Nano Lett. 7 (2007) 3296–3299.
[34] S.B. Yin, P.K. Shen, S.Q. Song, S.P. Jiang, Electrochim. Acta 54 (2009) 6954–6958.
[35] Y.L. Li, F.P. Hu, X. Wang, P.K. Shen, Electrochem. Commun. 10 (2008) 1101–1104.
[36] P.K. Shen, Z.Q. Tian, Electrochim. Acta 49 (2004) 3107–3111.
[37] C.W. Xu, L.Q. Cheng, P.K. Shen, Y.L. Liu, Electrochem. Commun. 9 (2007) 997–1001.
[38] F.P. Hu, Z.Y. Wang, Y.L. Li, C.M. Li, X. Zhang, P.K. Shen, J. Power Sources 177 (2008) 61–66.
[39] F.P. Hu, F.W. Ding, S.Q. Song, P.K. Shen, J. Power Sources 163 (2006) 415–419.
[40] Z.Y. Wang, F.P. Hu, P.K. Shen, Electrochem. Commun. 8 (2006) 1764–1768.
[41] G. Wu, G.F. Cui, D.Y. Li, P.K. Shen, N. Li, J. Mater. Chem. 19 (2009) 6581–6589.
[42] P.K. Shen, C.W. Xu, Electrochem. Commun. 8 (2006) 184–188.
[43] F.P. Hu, P.K. Shen, J. Power Sources 173 (2007) 877–881.
[44] F.P. Hu, G.F. Cui, Z.D. Wei, P.K. Shen, Electrochem. Commun. 10 (2008) 1303–1306.
[45] C. Bianchini, V. Bambagioni, J. Filippi, A. Marchionni, F. Vizza, P. Bert, A. Tampucci, Electrochem. Commun. 11 (2009) 1077–1080.
[46] X. Fang, L.Q. Wang, P.K. Shen, G.F. Cui, C. Bianchini, J. Power Sources 195 (2010) 1375–1378.
[47] S.J. Ding, C.L. Zhang, M. Yang, X.Z. Qu, Y.F. Lu, Z.Z. Yang, Polymer 47 (2006) 8360–8366.
[48] A. Lashtabeg, J. Drennan, R. Knibbe, J.L. Bradley, G.Q. Lu, Micropor. Mesopor. Mater. 117 (2009) 395–401.
[49] X.H. Xia, J.P. Tu, J.Y. Xiang, X.H. Huang, X.L. Wang, X.B. Zhao, J. Power Sources 195 (2010) 2014–2022.